TPX2 as a prognostic biomarker and potential therapeutic target for malignant melanoma proliferation and metastasis

FUQI LI[1], RONGHUI YANG[2] and ZHIXIAN WU[3]

[1]The First School of Clinical Medicine, Guangdong Medical University, Zhanjiang, Guangdong 524023, P.R. China;
[2]Department of Plastic Surgery, Maoming People's Hospital, Maoming, Guangdong 525000, P.R. China;
[3]Department of Burn Surgery, Affiliated Hospital of Guangdong Medical University, Zhanjiang, Guangdong 524013, P.R. China

Received November 26, 2025; Accepted February 18, 2026

DOI: 10.3892/etm.2026.13177

Abstract. Malignant melanoma is an aggressive skin cancer with increasing incidence and poor prognosis after metastasis. Identifying key molecular drivers of melanoma progression is critical for developing novel therapeutic strategies. Therefore, in the present study, differential gene expression analysis was conducted on GSE98394 and The Cancer Genome Atlas-skin cutaneous melanoma datasets using 'limma' package and Gene Expression Profiling Interactive Analysis 2. Consistently dysregulated genes were intersected and subjected to Kaplan-Meier survival and Cox regression analyses. Functional assays, including reverse transcription-quantitative PCR, western blotting, MTT proliferation assay, wound healing, Transwell migration and small interfering (si)RNA-mediated targeting protein for Xklp2 (TPX2) knockdown assays, were performed in A375 and C32 melanoma cells and PIG1 melanocytes. Intersection of the two datasets revealed eight upregulated and five downregulated genes, and high TPX2 expression was significantly associated with short overall survival. TPX2 mRNA and protein levels were markedly higher in A375 cells than in PIG1 controls. *TPX2* silencing via siRNA reduced aurora kinase A mRNA and protein levels, inhibited cell proliferation and impaired cell migration in wound healing and Transwell assays. Overall, the integrated bioinformatics and experimental analyses identified *TPX2* as a potent oncogene promoting cell proliferation and migration, at least in part, via upregulation of aurora kinase A in melanoma. In conclusion, TPX2 may constitute a potential prognostic biomarker and therapeutic target for metastatic melanoma.

Correspondence to: Dr Zhixian Wu, Department of Burn Surgery, Affiliated Hospital of Guangdong Medical University, 57 Renmin Avenue South, Xiashan, Zhanjiang, Guangdong 524013, P.R. China
E-mail: zhixianwu@126.com

Abbreviations: AURKA, aurora kinase A; RT-qPCR, reverse transcription-quantitative polymerase chain reaction; siRNA, small interfering RNA; SKCM, skin cutaneous melanoma; TCGA, The Cancer Genome Atlas; UV, ultraviolet

Key words: malignant melanoma, targeting protein for Xklp2, AURKA, prognostic biomarker, proliferation, metastasis

Introduction

Malignant melanoma (MM), a tumor arising from the malignant transformation of melanocytes, is characterized by high tumorigenic potential. Over the past 30 years, the global incidence of metastatic melanoma has rapidly increased, resulting in a notable increase in mortality (1). Although the incidence of melanoma in China is relatively low, ~20,000 new cases are observed annually (2). Although early-stage melanoma is curable via wide local excision (3), it can invade the dermis within months, becoming life-threatening upon metastasis. Notably, approximately one-third of patients with advanced melanoma present with metastases to the lungs, liver or brain at the time of diagnosis (4). Overall, the 5-year survival rate is as high as 99% for patients with localized melanoma, but it decreases to 27.3% for those with distant metastases (5); therefore, metastatic melanoma is generally associated with a poor prognosis.

Melanoma pathogenesis involves a complex interplay among ultraviolet (UV)-induced DNA damage, genetic mutations (such as *BRAF* and *NRAS*) and dysregulated melanogenesis. UV radiation, particularly UVB, induces thymine dimers and reactive oxygen species, leading to oxidative DNA damage and activation of oncogenic pathways, such as the p53 and melanocyte-inducing transcription factor-dependent melanin synthesis pathways (6-8). Although melanin protects against UV radiation, its intermediates can leak from melanosomes under pathological conditions, promoting tumor progression by enhancing hypoxia-inducible factor 1α-driven angiogenesis, metabolic reprogramming and immunosuppression (9,10). This dual role of melanogenesis underscores its potential as a therapeutic target. Therefore, systematic investigation of the pathogenesis and progression mechanisms of melanoma using various experimental approaches has marked theoretical and clinical value. Specifically, bioinformatics enables the analysis of melanoma-related genes and signaling pathways from large-scale data, revealing key molecular networks involved in pathogenesis and progression and providing precise targets for subsequent experimental research. Therefore, the present study

aimed to integrate public transcriptomic datasets from Gene Expression Omnibus and The Cancer Genome Atlas (TCGA) to identify high-confidence differentially expressed genes (DEGs) and prioritize candidates associated with melanoma prognosis, validate the expression and prognostic significance of targeting protein for Xklp2 (TPX2) in independent cohorts, and functionally characterize the role of TPX2 in melanoma cell proliferation and migration *in vitro* and define its regulatory relationship with aurora kinase A (AURKA) to evaluate TPX2 as a potential prognostic biomarker and therapeutic target.

Materials and methods

Bioinformatics analysis. MM-related gene expression data were retrieved from the Gene Expression Omnibus database of the National Center for Biotechnology Information (https://www.ncbi.nlm.nih.gov/geo/) using 'melanoma' as the search term. The GSE98394 (11) dataset (platform GPL16791) containing 27 commonly acquired nevus (normal control) and 51 primary melanoma samples was obtained and used for analysis. Differential analysis was conducted using the R package 'limma' v3.50.0 (https://bioinf.wehi.edu.au/limma/). Statistical significance of the differences between normal and tumor samples was analyzed via unpaired t-test (for normally distributed data) or Wilcoxon rank-sum test (for non-normally distributed data), with adjusted $P<1x10^{-10}$ and |fold change (FC)|>4 as thresholds. The R package 'pheatmap' v1.0.12 (https://CRAN.R-project.org/package=pheatmap) was used to generate a heatmap with hierarchical clustering, and a scatter plot was constructed to observe the expression levels and trends of DEGs. DEGs identified by limma were subjected to functional enrichment analysis to identify over-represented Gene Ontology categories (biological processes, cellular components and molecular functions) and Kyoto Encyclopedia of Genes and Genomes pathways (12,13). Enrichment results were summarized and visualized using the R package 'ggplot2' v4.0.1 (https://CRAN.R-project.org/package=ggplot2).

The mRNA-sequencing and gene mutation data of 469 skin cutaneous melanoma (SKCM) and 558 normal tissue samples were obtained from TCGA-SKCM dataset (https://tcga-data.nci.nih.gov/). Statistical analyses were conducted using Gene Expression Profiling Interactive Analysis 2 (http://gepia2.cancer-pku.cn), with adjusted $P<1x10^{-8}$ and |FC|>2 as thresholds. Gene expression values were presented as transcripts per million. Significantly upregulated and downregulated genes in the GSE98394 and TCGA-SKCM datasets were separately intersected to obtain the final lists of consistently upregulated and downregulated genes. Kaplan-Meier survival curves were generated to compare survival outcomes between groups, and statistical significance was assessed using the log-rank (Mantel-Cox) test. Hazard ratios (HRs) and corresponding 95% confidence intervals were calculated using Cox proportional hazards regression models. Genes significantly associated with patient survival were identified as candidates for further investigation.

To validate TPX2 expression and its association with melanoma progression, two independent datasets (GSE3189 and GSE46517) were retrieved from the Gene Expression Omnibus database. The GSE3189 (14) and GSE46517 (15) datasets were used to validate differential TPX2 expression between melanoma and nevus tissues. Statistical significance was assessed via unpaired t-tests for comparisons between two groups. For prognostic validation, the GSE65904 dataset was used to analyze the association between gene expression and disease-specific survival. Optimal cut-off points for separating high and low expression groups were determined using the survive_cutpoint function in the R package 'survminer'. Kaplan-Meier survival curves were generated, and differences were assessed using the log-rank test. Additionally, multivariate Cox proportional hazards regression models were constructed to evaluate the independent prognostic value of TPX2 and AURKA, adjusting for clinical covariates including age, sex and tumor stage.

Cell lines and culture. Human MM cells (A375 and C32) and immortalized human melanocytes (PIG1) originally from LMAI were provided by another laboratory at Guangdong Medical University (Zhanjiang, China). All cells were cultured in RPMI-1640 medium (Gibco; Thermo Fisher Scientific, Inc.) with 10% FBS (Shanghai ExCell Biology, Inc.) and 1% penicillin/streptomycin (Gibco; Thermo Fisher Scientific, Inc.) at 37˚C in a constant temperature incubator with 5% CO_2.

Reverse transcription-quantitative PCR (RT-qPCR). RNA was extracted from cells using TRIzol® (Invitrogen; Thermo Fisher Scientific, Inc.) and reverse-transcribed into cDNA (incubation at 50˚C for 15 min followed by 85˚C for 2 min) using HiScript II Q RT SuperMix for qPCR (Vazyme Biotech Co., Ltd.). RT-qPCR was performed using ChamQ Universal SYBR qPCR Master Mix (Vazyme Biotech Co., Ltd.) on the Bio-Rad CFX Opus 96 system (Bio-Rad Laboratories, Inc.). The thermocycling conditions were as follows: Initiation with a hot-start activation at 95˚C for 30 sec, followed by 40 cycles of a two-step amplification program consisting of denaturation at 95˚C for 10 sec and a combined annealing/extension step at 60˚C for 30 sec. Fluorescence signal acquisition was performed at the end of each 60˚C phase. To confirm the specificity of the amplified products and the absence of primer-dimers, a melting curve analysis was conducted immediately following the final cycle (60-95˚C). Relative gene expression was calculated using the $2^{-\Delta\Delta Cq}$ method (16), with GAPDH as the endogenous control for normalization. All experiments were independently repeated three times. The following primer sequences were used in the present study: *TPX2* forward, 5'-GAGGGCCTT TCTGGTTCTCT-3'; *TPX2* reverse, 5'-CTCCTGTAGTCT GGCCTCCT-3'; *GAPDH* forward, 5'-GTCTCCTCTGACTTC AACAGCG-3'; and *GAPDH* reverse, 5'-ACCACCCTGTTG CTGTAGCCAA-3'.

Western blotting. Proteins were extracted using RIPA buffer (Beyotime Biotechnology) with a protease inhibitor (P6730; Beijing Solarbio Science & Technology Co., Ltd.). The BCA assay (Beyotime Biotechnology) was used for protein quantification, and 20 μg total protein was loaded per lane. SDS-PAGE was used to separate proteins, which were transferred to PVDF membranes (MilliporeSigma). After blocking with 5% skimmed milk (Beyotime Biotechnology) for 1 h at room temperature, the membranes were incubated overnight with primary antibodies, including anti-TPX2 (dilution, 1:5,000;

cat. no. 11741-1-AP; Proteintech Group, Inc.), anti-AURKA (dilution, 1:2,000; cat. no. 66757-1-Ig; Proteintech Group, Inc.) and anti-GAPDH (dilution, 1:50,000; cat. no. 60004-1-Ig; Proteintech Group, Inc.) antibodies, at 4˚C. The membranes were further washed with 1X TBS with 0.05% Tween-20 (Beyotime Biotechnology) and incubated with goat anti-rabbit secondary antibodies (dilution, 1:5,000; cat. no. RGAR001; Proteintech Group, Inc.) or goat anti-mouse secondary antibodies (dilution, 1:5,000; cat. no. RGAM001; Proteintech Group, Inc.) at room temperature for 1 h. Protein bands were visualized using an enhanced chemiluminescence detection reagent (Thermo Fisher Scientific, Inc.). Band intensities were semi-quantified via densitometric analysis using ImageJ software v1.53 (National Institutes of Health). All experiments were independently repeated three times.

MTT assay. Cells were seeded in a 96-well plate (Thermo Fisher Scientific, Inc.) at a density of $1x10^3$ cells/well and cultured for 0, 12, 24, 36 and 48 h. An MTT solution (Beyotime Biotechnology) was used to assess cell viability. Formazan crystals were dissolved in DMSO (Thermo Fisher Scientific, Inc.), and the absorbance [optical density (OD)] was measured at 490 nm using a microplate reader. All experiments were independently repeated three times.

Wound healing assay. The wound healing assay was performed on cells grown to 90% confluence in a 6-well plate (Thermo Fisher Scientific, Inc.). Cells were cultured in RPMI-1640 medium (Gibco; Thermo Fisher Scientific, Inc.) with 10% FBS (Shanghai ExCell Biology, Inc.) and 1% penicillin/streptomycin (Gibco; Thermo Fisher Scientific, Inc.) at 37˚C in a constant temperature incubator with 5% CO_2. To establish a uniform wound, the cells were scraped with a 200-μl micropipette tip. After washing with phosphate-buffered saline, the cells were cultured with 2% FBS RPMI-1640 medium. Cell migration was observed using an inverted fluorescence microscope at 0 and 24 h. Wound closure was quantitatively assessed by measuring the wound area at 0 and 24 h using ImageJ software v1.53 (National Institutes of Health). The percentage of wound closure was calculated as follows: Healing rates (%)=[(initial wound width-wound width at 24 h)/initial wound width] x100. All measurements were performed in at least three randomly selected fields per well, and the mean value was used for statistical analysis. All experiments were independently repeated three times.

Transwell assay. A serum-free cell suspension containing $1x10^5$ cells was seeded in the upper chamber of a Transwell system (8.0 μm; Corning, Inc.), and culture medium with 10% fetal bovine serum was added to the lower chamber. After incubation at 37˚C in a constant temperature incubator with 5% CO_2 for 24 h, non-migrated cells on the upper surface of the membrane were gently removed, and the cells that had migrated to the lower surface of the filter were fixed with 4% paraformaldehyde for 30 min at room temperature, stained with crystal violet for 10 min at room temperature (Beyotime Biotechnology), washed with phosphate-buffered saline and allowed to dry. Then, the number of migrating cells was determined using an inverted microscope. All experiments were independently repeated three times.

Small interfering RNA (siRNA) transfection. A total of $5x10^5$ A375 and C32 cells were seeded in a 6-well plate at a density of 70-90%. *TPX2* siRNA (sense, 5'-AUUAUUAGCCUUAGUAAUGUA-3' and antisense, 5'-UACAUUACUAAGGCUAAUAAU-3') and siNC (sense, 5'-UUCUCCGAACGUGUCACGU-3' and antisense, 5'-ACGUGACACGUUCGGAGAA-3') were obtained from Changzhou Ruibo Bio-Technology Co., Ltd. siRNA (50 pmol) was transfected into the cells using the Lipofectamine® RNAiMAX reagent (Invitrogen; Thermo Fisher Scientific, Inc.). siRNA-lipid complexes were prepared in serum-free medium and added to cells, which were then incubated at 37˚C in a humidified atmosphere with 5% CO_2 for 6 h. Subsequently, the transfection medium was replaced with complete culture medium. Cells were harvested for RT-qPCR and western blot analyses 48 h after transfection. Functional assays were performed at the following intervals after transfection unless otherwise stated: MTT assays at 0, 12, 24, 36 and 48 h, and wound healing and Transwell migration assays at 24 h. Cells transfected with non-targeting siNC were used as negative controls for all siRNA transfection experiments. Untransfected parental A375 and C32 cells were included as blank controls where indicated.

Statistical analyses. Data were analyzed using SPSS v22.0 (IBM, Corp.) and are presented as the mean ± standard deviation. GraphPad Prism v8.0 (Dotmatics) was used for data visualization. Statistical analyses of quantitative data were conducted using one-way ANOVA. Levene's test and F-test were applied to test for unequal variances, and Welch's ANOVA was used for analysis when variances were unequal. Tukey's honestly significant difference test was used when Levene's test indicated equal variances. If Levene's test indicated unequal variances and Welch's ANOVA was applied, pairwise comparisons were performed using the Games-Howell post hoc test. $P<0.05$ was considered to indicate a statistically significant difference.

Results

Differential expression and functional enrichment analyses of the GSE98394 and TCGA-SKCM datasets. Differential expression analysis of the GSE98394 dataset identified 878 significantly downregulated and 812 significantly upregulated genes based on the thresholds of $|FC|>4$ and adjusted $P<1x10^{-10}$ (Fig. 1A and B). Functional enrichment analysis of these DEGs revealed significant involvement in pathways such as the 'cytokine-cytokine receptor interaction' and 'chemokine signaling pathway'. The enriched biological processes included 'leukocyte-mediated immunity', 'lymphocyte mediated immunity' and 'regulation of lymphocyte activation' (Fig. 1C and D). Similarly, analysis of TCGA-SKCM dataset using cut-offs of $|(FC)|>2$ and adjusted $P<1x10^{-8}$ identified 357 significantly downregulated and 67 significantly upregulated genes (Fig. 1E). Intersecting the DEGs from both datasets revealed eight potentially upregulated genes [anti-silencing function 1B histone chaperone, *TPX2*, transmembrane protein 132A, PDZ-binding kinase, von Willebrand factor, protein kinase membrane-associated tyrosine/threonine 1 (*PKMYT1*), ubiquitin-conjugating enzyme E2 C (*UBE2C*) and insulin-like

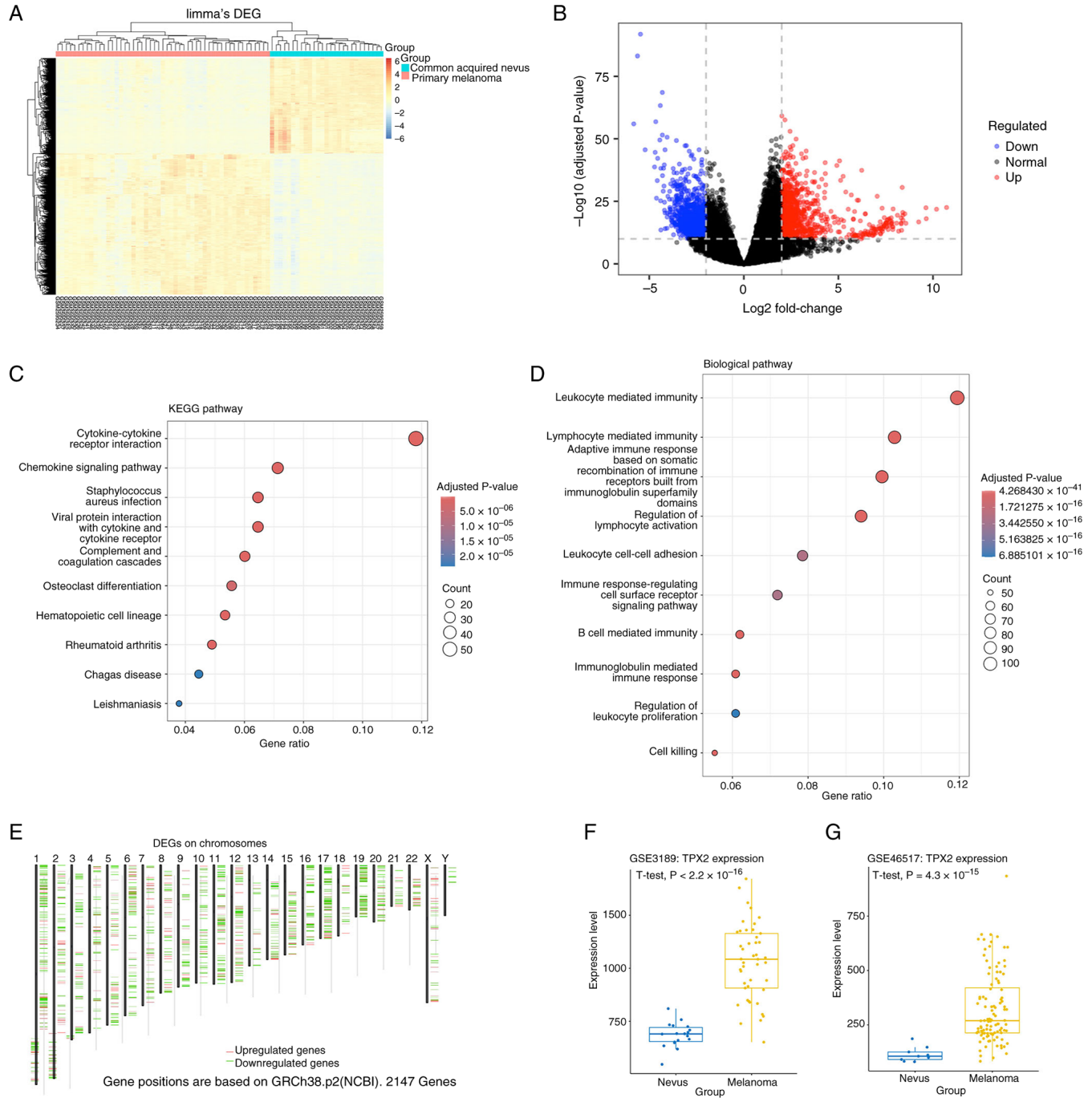

Figure 1. DEGs and functional enrichment analyses of tumor and normal samples. (A) Heatmap of DEGs showing distinct gene expression profiles in the GSE98394 dataset. Hierarchical clustering was performed using the top significantly upregulated and downregulated genes. (B) Volcano plot of DEGs from the GSE98394 dataset. Red dots indicate significantly upregulated genes, blue dots indicate significantly downregulated genes and black dots indicate genes with no significant changes. Vertical dashed lines represent |fold change|>4, whereas horizontal dashed lines indicate the threshold of adjusted P<1x10^{-10}. (C) KEGG pathway enrichment analysis of DEGs. The top 10 significantly enriched pathways are shown, with dot size indicating the number of genes and color indicating adjusted P-values. (D) Gene Ontology biological process enrichment analysis of DEGs. The top enriched immune-related biological processes are shown, with gene ratio on the x-axis and dot size representing gene counts. (E) Chromosomal distribution of DEGs from The Cancer Genome Atlas-skin cutaneous melanoma dataset. Upregulated genes are marked in red, whereas downregulated genes are indicated in green. All DEGs are mapped to their corresponding chromosomal locations. (F) Box plot of TPX2 expression in the GSE3189 dataset. (G) Box plot of TPX2 expression in the GSE46517 dataset. DEG, differentially expressed gene; KEGG, Kyoto Encyclopedia of Genes and Genomes; TPX2, targeting protein for Xklp2.

growth factor-2] and five potentially downregulated genes [adhesion G protein-coupled receptor V1, phytanoyl-CoA 2-hydroxylase-interacting protein, complement factor H (*CFH*), troponin C1 and family with sequence similarity 153 member B]. Moreover, *TPX2* mRNA levels were significantly higher in melanoma than in nevi (P<0.001) in the GSE3189 cohort (Fig. 1F). These findings were consistent with those obtained from the GSE46517 dataset, in which TPX2 levels were also significantly upregulated in malignant tissues (P<0.001; Fig. 1G). Across both validation cohorts, TPX2 expression demonstrated an ~2.8-fold increase in melanoma compared to that in benign lesions.

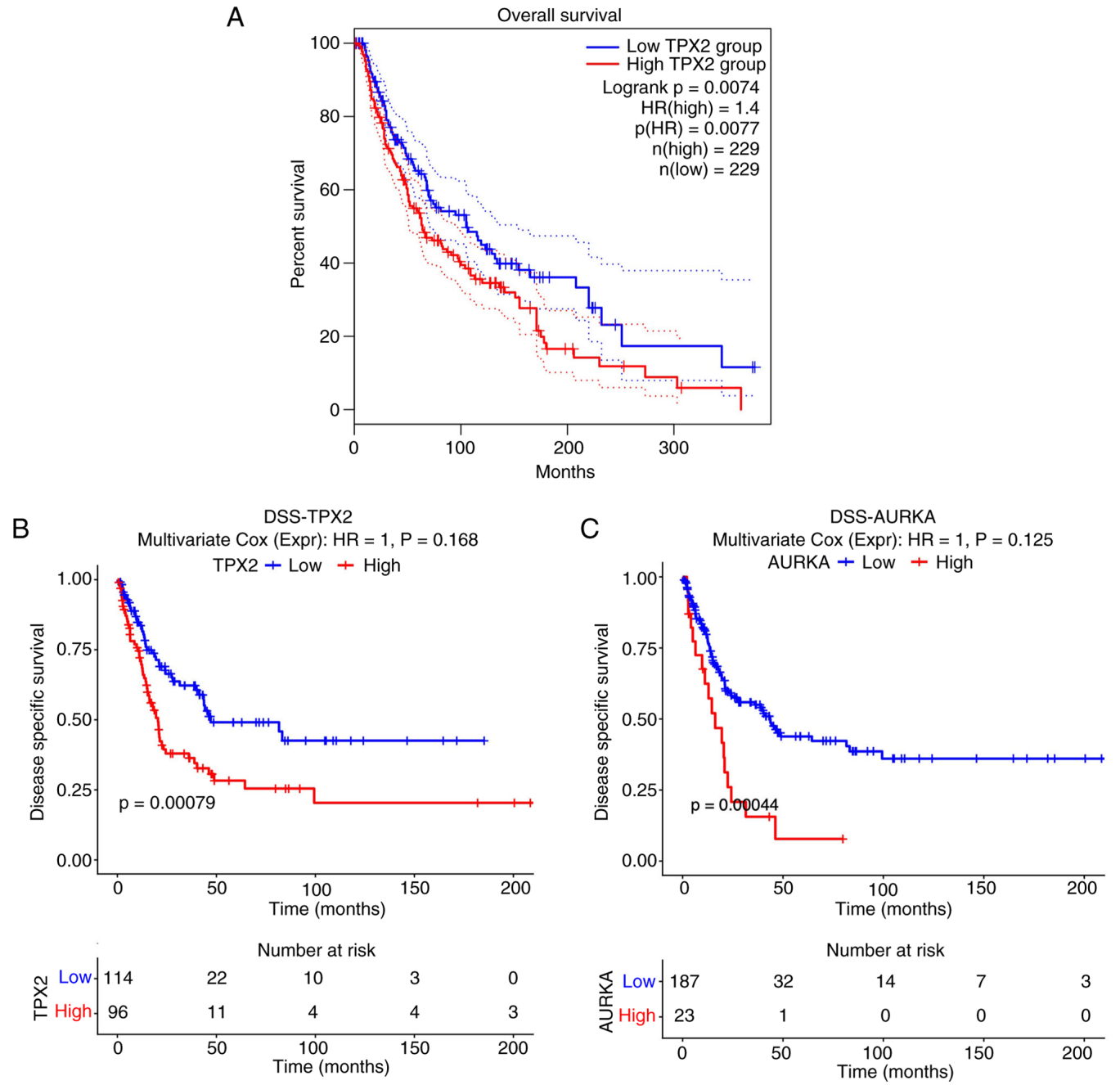

Figure 2. Kaplan-Meier survival analysis of candidate genes in patients with melanoma from The Cancer Genome Atlas cohort. (A) Patients with low TPX2 expression showed significantly longer overall survival than those with high TPX2 expression (log-rank P=0.0074; HR=1.4). Percentage survival was plotted over time (months), with 95% confidence intervals indicated by dotted lines. Grouping was based on median expression (n=229 for each group). Kaplan-Meier survival curves of DSS in the GSE65904 cohort stratified by (B) TPX2 and (C) AURKA expression. HR, hazard ratio; DSS, disease-specific survival; AURKA, aurora kinase A; TPX2, targeting protein for Xklp2.

Impact of candidate functional genes on patient overall survival (OS). To evaluate the prognostic significance of candidate genes in melanoma, Kaplan-Meier survival analyses were conducted using OS data from TCGA melanoma cohort. Patients were divided into high and low expression groups based on median expression levels. As shown in Fig. 2A, patients with low expression of TPX2 exhibited significantly longer OS compared with those with high expression (log-rank P=0.0074; HR=1.4), suggesting a potential oncogene function of TPX2 in melanoma. To further validate the prognostic value of the identified candidate genes, an independent survival analysis was performed using the GSE65904 dataset. Patients were stratified into high and low expression groups based on the optimal cut-off values for TPX2 and AURKA. Kaplan-Meier survival analysis revealed that high expression levels of both TPX2 and AURKA were significantly associated with poor disease-specific survival (log-rank P<0.001 for both; Fig. 2B and C). Specifically, patients in the high TPX2 expression group exhibited significantly lower survival probability than those in the low TPX2 expression group. Similarly, elevated AURKA expression was an indicator of unfavorable prognosis. The univariate and multivariate Cox regression

Table I. Univariate and multivariate cox regression analysis.

A, TPX2

Variable	Univariate HR (95% CI)	Univariate P-value	Multivariate HR (95% CI)	Multivariate P-value
High vs. low expression	1.938 (1.308-2.871)	<0.001	1.910 (1.273-2.866)	0.002
Age (continuous variable)	0.998 (0.985-1.012)	0.797	1.002 (0.987-1.016)	0.827
Sex (male vs. female)	1.335 (0.885-2.016)	0.169	1.170 (0.766-1.788)	0.468
Tumor stage (in-transit, local, primary and regional vs. 'general')	0.354 (0.204-0.613)	<0.001	0.374 (0.214-0.652)	<0.001

B, AURKA

Variable	Univariate HR (95% CI)	Univariate P-value	Multivariate HR (95% CI)	Multivariate P-value
High vs. low expression	2.440 (1.460-4.079)	<0.001	2.174 (1.284-3.682)	0.004
Age (continuous variable)	0.998 (0.985-1.012)	0.797	1.001 (0.986-1.015)	0.932
Sex (male vs. female)	1.335 (0.885-2.016)	0.169	1.278 (0.841-1.941)	0.250
Tumor stage (in-transit, local, primary and regional vs. 'general')	0.354 (0.204-0.613)	<0.001	0.391 (0.223-0.685)	0.001

AURKA, aurora kinase A; TPX2, targeting protein for Xklp2; HR, hazard ratio; CI, confidence interval.

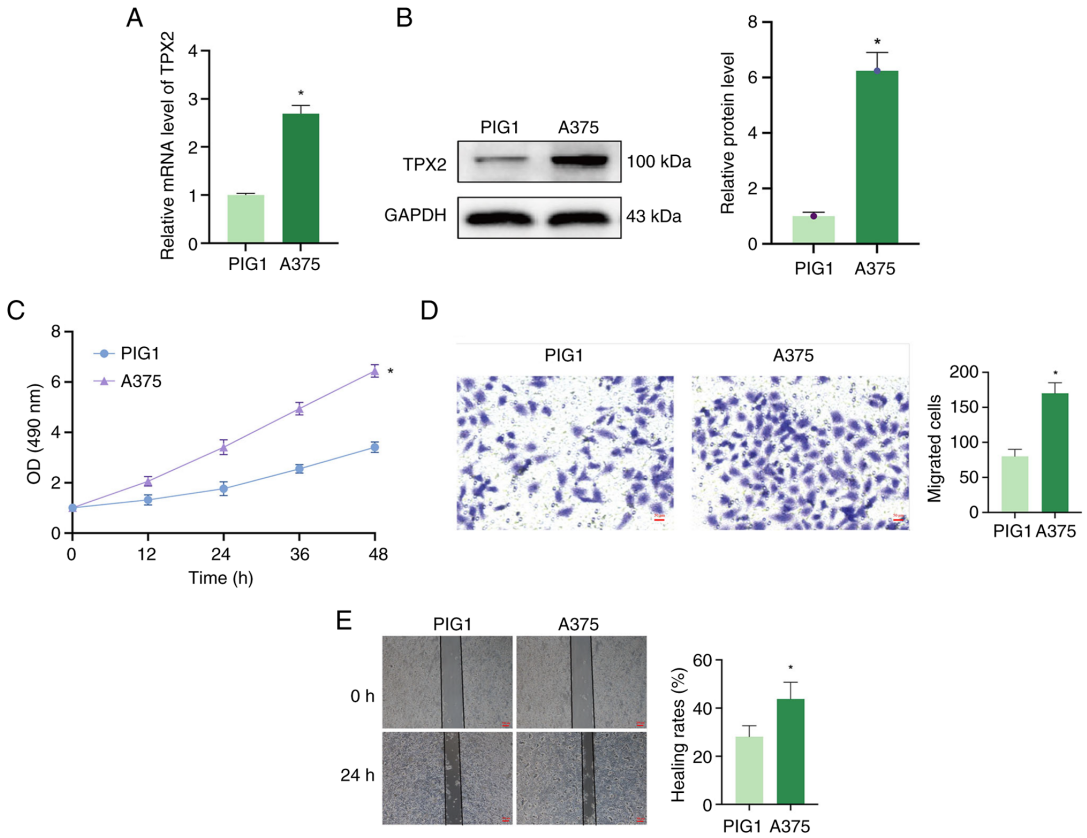

Figure 3. TPX2 is highly expressed in melanoma cells and promotes cell proliferation and migration. (A) Reverse transcription-quantitative PCR analysis of *TPX2* mRNA levels in normal melanocytes (PIG1) and melanoma cells (A375). (B) Western blot analysis of TPX2 protein levels in PIG1 and A375 cells. GAPDH was used as a loading control. (C) Cell proliferation was measured via MTT assay at 0, 12, 24, 36 and 48 h. A375 cells showed significantly higher proliferation rates than PIG1 cells. (D) Representative images of Transwell migration assay showing increased migration of A375 cells compared to that of PIG1 (magnification, x200; scale bar, 50 μm). (E) Wound healing assay showing faster closure of scratch wounds in A375 cells than in PIG1 cells at 24 h (magnification, x50; scale bar, 200 μm). Data are presented as the mean ± SD. *P<0.05 vs. PIG1. TPX2, targeting protein for Xklp2; OD, optical density.

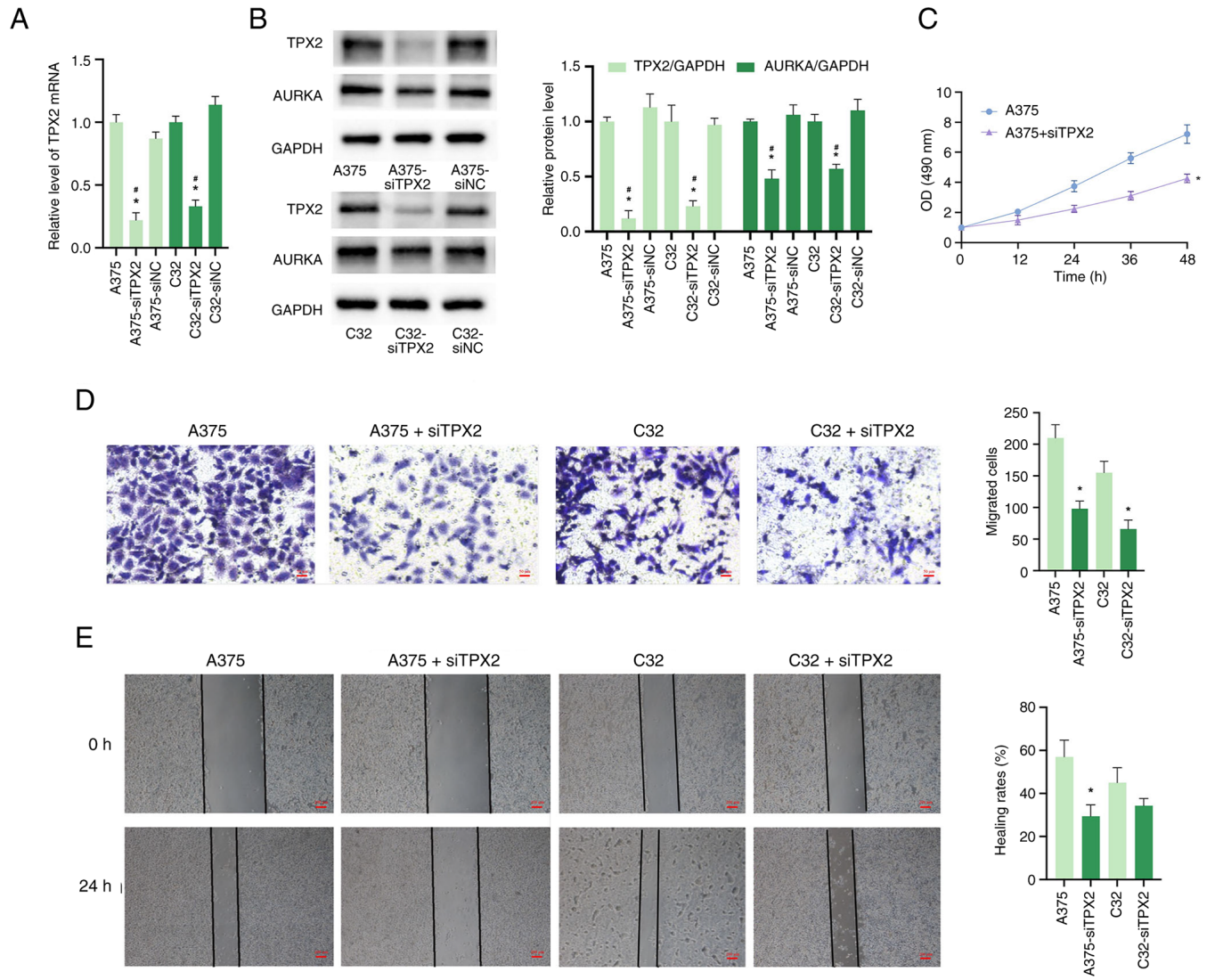

Figure 4. *TPX2* knockdown reduces AURKA expression and suppresses proliferation and migration in A375 and C32 melanoma cells. (A) Reverse transcription-quantitative PCR analysis of TPX2 mRNA levels in A375 and C32 cells transfected with siTPX2 or non-targeting siNC. Data are presented separately for each cell line. (B) Western blot analysis of TPX2 and AURKA protein levels in parental A375 and C32 cells and in the corresponding siTPX2- and siNC-transfected cells. GAPDH served as a loading control. (C) Cell proliferation assessed using an MTT assay at the indicated time points. Proliferation of siTPX2-transfected cells and parental controls is shown. (D) Transwell migration assay of A375 and C32 cells and their siTPX2 transfectants. Migrated cells were stained and counted under a microscope (magnification, x200; scale bar, 50 μm). siTPX2-transfected cells were compared with parental cells within each cell line. (E) Wound healing assay images at 0 and 24 h. Wound closure was quantified and siTPX2 transfectants were compared with parent cell controls (magnification, x50; scale bar, 200 μm). Data are presented as the mean ± SD. *P<0.05 vs. parental cells, $^{\#}$P<0.05 vs. siNC, A375 or C32 as applicable. si, small interfering; NC, negative control; AURKA, aurora kinase A; TPX2, targeting protein for Xklp2; OD, optical density.

results are shown in Table I. These results from an independent cohort further confirm that TPX2 and AURKA are reliable biomarkers for predicting survival outcomes in patients with melanoma.

TPX2 promotes the growth and migration of A375 melanoma cells. To evaluate the differential expression of TPX2 between normal melanocytes and melanoma cells, *TPX2* mRNA levels were assessed in PIG1 and A375 cells. RT-qPCR analysis revealed that *TPX2* mRNA expression was significantly higher in A375 cells than in PIG1 cells (P<0.05; Fig. 3A). This upregulation was further confirmed at the protein level via western blotting, which showed greater TPX2 protein expression in A375 cells compared with PIG1 cells (P<0.05; Fig. 3B). To investigate whether elevated TPX2 expression is associated with functional alterations in melanoma cells, the migration and proliferation of A375 and PIG1 cells were evaluated. MTT proliferation assays indicated that A375 cells exhibited significantly higher OD values from 12 to 48 h, indicating greater proliferation compared with PIG1 cells (P<0.05; Fig. 3C). Additionally, Transwell migration assays demonstrated that A375 cells exhibited significantly enhanced migration, as indicated by a higher number of A375 cells traversing the membrane compared with PIG1 cells (P<0.05; Fig. 3D). Consistently, wound healing assays revealed that A375 cells migrated more rapidly, with a noticeably smaller wound area at 24 h (P<0.05; Fig. 3E). Collectively, these findings suggested that TPX2 is highly expressed in A375 melanoma cells and may be associated with melanoma progression by promoting cell proliferation and migration.

TPX2 knockdown inhibits AURKA expression and attenuates the proliferation and migration of melanoma cells. To further investigate the functional roles of TPX2 in melanoma cells, siRNA-mediated knockdown of *TPX2* in melanoma cells was performed. RT-qPCR analysis confirmed a significant reduction in *TPX2* mRNA levels after transfection with TPX2-specific siRNA compared with those in control A375 cells ($P<0.05$; Fig. 4A). Western blotting analysis further validated the decrease in TPX2 protein levels in A375-siTPX2 and C32-siTPX2 cells and revealed a concomitant reduction in AURKA protein levels ($P<0.05$; Fig. 4B). Functionally, MTT assays demonstrated that TPX2 knockdown significantly inhibited A375 cell proliferation. The A375-siTPX2 group exhibited markedly lower OD values than the control A375 group at all time points ($P<0.05$; Fig. 4C). Transwell migration assays showed that the number of migrated cells was significantly reduced in the A375-siTPX2 and C32-siTPX2 groups, indicating impaired migration ($P<0.05$; Fig. 4D). Consistently, wound healing assays revealed that the scratch area remained largely open in *TPX2*-silenced cells after 24 h, whereas A375 and C32 cells exhibited notable wound closure ($P<0.05$ for A375 cells; Fig. 4E). Collectively, these results suggested that TPX2 promotes melanoma cell proliferation and migration, which could be related to AURKA upregulation.

Discussion

MM remains a challenging malignancy with limited therapeutic options, particularly in advanced stages (17). Melanoma arises from melanocytes, which are responsible for melanin production and predominantly located in the skin but also found in mucosal tissues, eyes and other organs (18). Globally, over 324,635 new melanoma cases and 57,043 deaths were reported in 2020, with cutaneous melanoma being dominant in white populations (>90%) and acral subtypes being more common in East Asian populations (19). The present study integrated bioinformatics analysis with functional experiments to identify key molecular drivers of melanoma progression, focusing on the oncogenic role of TPX2 and its interplay with AURKA. The present findings revealed TPX2 as a notable regulator of melanoma cell proliferation and migration, highlighting it as a novel therapeutic target.

The intersection of DEGs from the GSE98394 and TCGA-SKCM datasets identified *TPX2*, *UBE2C* and *PKMYT1* as consistently upregulated genes. These genes are implicated in mitotic regulation and cell cycle progression, processes frequently dysregulated in cancer (20-22). Notably, TPX2, a microtubule-associated protein essential for spindle assembly, drives genomic instability and metastasis in various cancers (20). Consistently, the present survival analysis revealed that high TPX2 expression was associated with shorter OS in patients with melanoma. This aligns with previous reports linking TPX2 to aggressive phenotypes in hepatocellular carcinoma (23) and breast cancer (24), suggesting a conserved oncogenic role across malignancies.

Clinically, early-stage melanoma is curable with surgery; however, metastatic disease has a poor 5-year survival rate of 27.3% (5). Traditional chemotherapy, such as dacarbazine and temozolomide, shows limited efficacy (10-20% response rates) and marked toxicity (25-27). Advances in targeted therapies (BRAF/MEK inhibitors) and immunotherapies (anti-cytotoxic T-lymphocyte-associated protein-4 and anti-programmed death protein-1 antibodies, as well as oncolytic viruses such as Talimogene laherparepvec) have improved outcomes in patients with BRAF-mutant and advanced melanoma (28-31). However, drug resistance and immune-related adverse events remain major obstacles. The identification of TPX2 as a driver of cell proliferation and migration in the present study adds to the existing molecular toolkit for addressing these challenges.

Functional validation revealed that *TPX2* silencing significantly impaired melanoma cell proliferation and migration. Notably, *TPX2* knockdown concurrently reduced AURKA expression at the protein level. AURKA, a serine/threonine kinase critical for mitotic entry, is often co-amplified with TPX2 in cancer (32,33). TPX2 primarily stabilizes AURKA by binding to it, recruiting it to microtubules and protecting it from degradation, thereby indirectly contributing to high AURKA levels by increasing its stability and activation (34,35). Furthermore, AURKA is a driver of epithelial-mesenchymal transition and metastasis, linking TPX2 to melanoma aggressiveness (36). This interaction may underpin the mitotic defects and reduced migration observed in TPX2-depleted cells. Although TPX2 is well characterized as a physical scaffold that stabilizes AURKA and protects it from degradation, its contribution to downstream cellular phenotypes remains to be fully elucidated (37). The reduction in transcript abundance does not necessarily imply a direct transcriptional role of TPX2. Instead, it possibly reflects an indirect consequence of G_2/M phase or cell cycle arrest typically observed following TPX2 depletion (38). Because AURKA expression is strictly regulated by the cell cycle, peaking during the late G_2 and early M phases, a shift in the cell cycle profile toward G_1/S possibly results in lower steady-state *AURKA* mRNA levels (39). However, the precise molecular association between TPX2 and AURKA warrants further investigation, including chromatin immunoprecipitation, promoter activity and pull-down assays, to determine the mechanisms by which TPX2 regulates AURKA transcription and protein translation.

To the best of our knowledge, the present study is the first to demonstrate that TPX2 not only drives melanoma cell proliferation but also directly enhances cell migration, potentially via AURKA-dependent pathways. This dual functionality positions TPX2 as a coordinator of melanoma progression, bridging cell cycle dysregulation and metastatic potential. The association between TPX2 overexpression and poor survival in TCGA-SKCM cohort further underscores the clinical relevance of TPX2 as a prognostic biomarker. However, this study has several limitations: First, experimental validation focused solely on TPX2 in the A375 and C32 cell lines, necessitating further studies on other melanoma models (such as BRAF/NRAS-mutant cell lines) and *in vivo* systems to validate the findings. Second, the mechanism linking TPX2 to AURKA regulation remains unclear. Lastly, although bioinformatics analysis prioritized high-confidence DEGs, functional studies on other candidates (*PKMYT1* and *UBE2C*) are necessary to determine their contributions to melanoma progression.

In summary, the present integrated approach identified *TPX2* as a key oncogene driving melanoma proliferation and migration, potentially via AURKA upregulation. The present findings suggested that TPX2 may be both a prognostic

biomarker and potential therapeutic target. Future studies should evaluate TPX2 inhibition in preclinical models and investigate combinatorial strategies targeting TPX2 and AURKA or melanogenesis pathways to mitigate melanoma aggressiveness and enhance the efficacy of existing immunotherapies and targeted therapies.

Acknowledgements

Not applicable.

Funding

The present study was supported by the Guangdong Province Medical Science Research Project (grant no. A2019103).

Availability of data and materials

The data generated in the present study may be requested from the corresponding author.

Authors' contributions

FL conceptualized the study, designed the methodology, performed bioinformatics analysis and the experiments, and wrote the original draft of the manuscript. RY generated figures, was involved in validation, and performed formal analysis, bioinformatics analysis and the experiments. ZW conceptualized the study, acquired funding and reviewed the manuscript. FL and RY confirm the authenticity of all the raw data. All authors have read and approved the final version of the manuscript.

Ethics approval and consent to participate

Not applicable.

Patient consent for publication

Not applicable.

Competing interests

The authors declare that they have no competing interests.

References

1. Siegel RL, Giaquinto AN and Jemal A: Cancer statistics, 2024. CA Cancer J Clin 74: 12-49, 2024.
2. Xu L, Cheng Z, Cui C, Wu X, Yu H, Guo J and Kong Y: Frequent genetic aberrations in the cell cycle related genes in mucosal melanoma indicate the potential for targeted therapy. J Transl Med 17: 245, 2019.
3. Kozovska Z, Gabrisova V and Kucerova L: Malignant melanoma: Diagnosis, treatment and cancer stem cells. Neoplasma 63: 510-517, 2016.
4. Luke JJ, Flaherty KT, Ribas A and Long GV: Targeted agents and immunotherapies: Optimizing outcomes in melanoma. Nat Rev Clin Oncol 14: 463-482, 2017.
5. Herndon TM, Demko SG, Jiang X, He K, Gootenberg JE, Cohen MH, Keegan P and Pazdur R: U.S. Food and drug administration approval: Peginterferon-alfa-2b for the adjuvant treatment of patients with melanoma. Oncologist 17: 1323-1328, 2012.
6. Slominski A, Tobin DJ, Shibahara S and Wortsman J: Melanin pigmentation in mammalian skin and its hormonal regulation. Physiol Rev 84: 1155-1228, 2004.
7. dos Santos Videira IF, Moura DF and Magina S: Mechanisms regulating melanogenesis. An Bras Dermatol 88: 76-83, 2013.
8. Garmyn M, Young AR and Miller SA: Mechanisms of and variables affecting UVR photoadaptation in human skin. Photochem Photobiol Sci 17: 1932-1940, 2018.
9. Slominski RM, Sarna T, Plonka PM, Raman C, Brozyna AA and Slominski AT: Melanoma, melanin, and melanogenesis: The Yin and Yang relationship. Front Oncol 12: 842496, 2022.
10. Slominski AT, Zmijewski MA, Plonka PM, Szaflarski JP and Paus R: How UV light touches the brain and endocrine system through skin, and why. Endocrinology 159: 1992-2007, 2018.
11. Badal B, Solovyov A, Di Cecilia S, Chan JM, Chang LW, Iqbal R, Aydin IT, Rajan GS, Chen C, Abbate F, *et al*: Transcriptional dissection of melanoma identifies a high-risk subtype underlying TP53 family genes and epigenome deregulation. JCI Insight 2: e92102, 2017.
12. Kanehisa M and Goto S: KEGG: Kyoto encyclopedia of genes and genomes. Nucleic Acids Res 28: 27-30, 2000.
13. Ashburner M, Ball CA, Blake JA, Botstein D, Butler H, Cherry JM, Davis AP, Dolinski K, Dwight SS, Eppig JT, *et al*: Gene ontology: tool for the unification of biology. The gene ontology consortium. Nat Genet 25: 25-29, 2000.
14. Talantov D, Mazumder A, Yu JX, Briggs T, Jiang Y, Backus J, Atkins D and Wang Y: Novel genes associated with malignant melanoma but not benign melanocytic lesions. Clin Cancer Res 11: 7234-7242, 2005.
15. Kabbarah O, Nogueira C, Feng B, Nazarian RM, Bosenberg M, Wu M, Scott KL, Kwong LN, Xiao Y, Cordon-Cardo C, *et al*: Integrative genome comparison of primary and metastatic melanomas. PLoS One 5: e10770, 2010.
16. Livak KJ and Schmittgen TD: Analysis of relative gene expression data using real-time quantitative PCR and the 2(-Delta Delta C(T)) method. Methods 25: 402-408, 2001.
17. Zavaleta-Monestel E, Quesada-Villaseñor R, Barrantes-López M, Arguedas-Chacón S, Campos-Hernández J, Rojas-Chinchilla C, García-Montero J, Castro-Ulloa J, Anchía-Alfaro A and Montenegro-Chaves JR: Advancements in the treatment of multiple myeloma. Cureus 16: e74970, 2024.
18. Jitian Mihulecea CR and Rotaru M: Review: The key factors to melanomagenesis. Life (Basel) 13: 181, 2023.
19. Sung H, Ferlay J, Siegel RL, Laversanne M, Soerjomataram I, Jemal A and Bray F: Global cancer statistics 2020: GLOBOCAN estimates of incidence and mortality worldwide for 36 cancers in 185 countries. CA Cancer J Clin 71: 209-249, 2021.
20. Aguirre-Portoles C, Bird AW, Hyman A, Canamero M, Perez de Castro I and Malumbres M: Tpx2 controls spindle integrity, genome stability, and tumor development. Cancer Res 72: 1518-1528, 2012.
21. Zhang S, You X, Zheng Y, Shen Y, Xiong X and Sun Y: The UBE2C/CDH1/DEPTOR axis is an oncogene and tumor suppressor cascade in lung cancer cells. J Clin Invest 133: e162434, 2023.
22. Wang S, Xiong Y, Luo Y, Shen Y, Zhang F, Lan H, Pang Y, Wang X, Li X, Zheng X, *et al*: Genome-wide CRISPR screens identify PKMYT1 as a therapeutic target in pancreatic ductal adenocarcinoma. EMBO Mol Med 16: 1115-1142, 2024.
23. Wang Y, Wang H, Yan Z, Li G, Hu G, Zhang H, Huang D, Wang Y, Zhang X, Yan Y, *et al*: The critical role of dysregulated Hh-FOXM1-TPX2 signaling in human hepatocellular carcinoma cell proliferation. Cell Commun Signal 18: 116, 2020.
24. Marugán C, Sanz-Gómez N, Ortigosa B, Monfort-Vengut A, Bertinetti C, Teijo A, González M, Alonso de la Vega A, Lallena MJ, Moreno-Bueno G and de Cárcer G: TPX2 overexpression promotes sensitivity to dasatinib in breast cancer by activating YAP transcriptional signaling. Mol Oncol 18: 1531-1551, 2024.
25. Jiang G, Li RH, Sun C, Liu YQ and Zheng JN: Dacarbazine combined targeted therapy versus dacarbazine alone in patients with malignant melanoma: a meta-analysis. PLoS One 9: e111920, 2014.
26. Middleton MR, Grob JJ, Aaronson N, Fierlbeck G, Tilgen W, Seiter S, Gore M, Aamdal S, Cebon J, Coates A, *et al*: Randomized phase III study of temozolomide versus dacarbazine in the treatment of patients with advanced metastatic malignant melanoma. J Clin Oncol 18: 158-166, 2000.

27. Guven K, Kittler H, Wolff K and Pehamberger H: Cisplatin and carboplatin combination as second-line chemotherapy in dacarbazine-resistant melanoma patients. Melanoma Res 11: 411-415, 2001.
28. Larkin J, Del Vecchio M, Mandalá M, Gogas H, Arance Fernandez AM, Dalle S, Cowey CL, Schenker M, Grob JJ, Chiarion-Sileni V, *et al*: Adjuvant nivolumab versus ipilimumab in resected stage III/IV melanoma: 5-year efficacy and biomarker results from CheckMate 238. Clin Cancer Res 29: 3352-3361, 2023.
29. Eggermont AMM, Blank CU, Mandala M, Long GV, Atkinson V, Dalle S, Haydon A, Lichinitser M, Khattak A, Carlino MS, *et al*: Adjuvant pembrolizumab versus placebo in resected stage III melanoma. N Engl J Med 378: 1789-1801, 2018.
30. Eggermont AM, Suciu S, Santinami M, Testori A, Kruit WH, Marsden J, Punt CJ, Salès F, Gore M, MacKie R, *et al*: Adjuvant therapy with pegylated interferon alfa-2b versus observation alone in resected stage III melanoma: Final results of EORTC 18991, a randomised phase III trial. Lancet 372: 117-126, 2008.
31. Ott PA, Hu Z, Keskin DB, Shukla SA, Sun J, Bozym DJ, Zhang W, Luoma A, Giobbie-Hurder A, Peter L, *et al*: An immunogenic personal neoantigen vaccine for patients with melanoma. Nature 547: 217-221, 2017.
32. Holder J, Miles JA, Batchelor M, Popple H, Walko M, Yeung W, Kannan N, Wilson AJ, Bayliss R and Gergely F: CEP192 localises mitotic Aurora-A activity by priming its interaction with TPX2. EMBO J 43: 5381-5420, 2024.
33. Li H, Wang Y, Lin K, Venkadakrishnan VB, Bakht M, Shi W, Meng C, Zhang J, Tremble K, Liang X, *et al*: CHD1 promotes sensitivity to aurora kinase inhibitors by suppressing interaction of AURKA with its coactivator TPX2. Cancer Res 82: 3088-3101, 2022.
34. Bayliss R, Sardon T, Vernos I and Conti E: Structural basis of Aurora-A activation by TPX2 at the mitotic spindle. Mol Cell 12: 851-862, 2003.
35. Eyers PA, Erikson E, Chen LG and Maller JL: A novel mechanism for activation of the protein kinase Aurora A. Curr Biol 13: 691-697, 2003.
36. Shen HM, Zhang D, Xiao P, Qu B and Sun YF: E2F1-mediated KDM4A-AS1 up-regulation promotes EMT of hepatocellular carcinoma cells by recruiting ILF3 to stabilize AURKA mRNA. Cancer Gene Ther 30: 1007-1017, 2023.
37. Polverino F, Mastrangelo A and Guarguaglini G: Contribution of AurkA/TPX2 overexpression to chromosomal imbalances and cancer. Cells 13: 1397, 2024.
38. Liu S, Cai J, Qian X, Zhang J, Zhang Y, Meng X, Wang M, Gao P and Zhong X: TPX2 lactylation is required for the cell cycle regulation and hepatocellular carcinoma progression. Life Sci Alliance 8: e202402978, 2025.
39. Vats P, Saini C, Baweja B, Srivastava SK, Kumar A, Kushwah AS and Nema R: Aurora kinases signaling in cancer: From molecular perception to targeted therapies. Mol Cancer 24: 180, 2025.